SPICE3 IMPLEMENTATION OF A NON-QUASI-STATIC MOSFET MODEL WITH LEVEL-2 DC MODEL

by

H. J. Park, P. K. Ko, and C. Hu

Memorandum No. UCB/ERL M89/70

8 June 1989

SPICE3 IMPLEMENTATION OF A NON-QUASI-STATIC MOSFET MODEL WITH LEVEL-2 DC MODEL

by

H. J. Park, P. K. Ko, and C. Hu

Memorandum No. UCB/ERL M89/70

8 June 1989

ELECTRONICS RESEARCH LABORATORY

College of Engineering
University of California, Berkeley
94720

SPICE3 IMPLEMENTATION OF A NON-QUASI-STATIC MOSFET MODEL WITH LEVEL-2 DC MODEL

by

H. J. Park, P. K. Ko, and C. Hu

Memorandum No. UCB/ERL M89/70

8 June 1989

ELECTRONICS RESEARCH LABORATORY

College of Engineering
University of California, Berkeley
94720

ABSTRACT

A NQS(Non-Quasi-Static) MOSFET charge model[1] with SPICE level-2 DC model[2] has been implemented in SPICE3.B.1. It includes the DC, AC and transient analyses. The DC model includes all the features of level-2 DC model.[2] Different model equations are used for AC and transient analyses. The model for the transient analysis is charge-based and it guarantees the charge conservation. Different model equations are used for AC and transient analyses. The model for the transient analysis is charge-based and it guarantees the charge conservation. This model is based on the charge sheet formulation[1], and includes the channel transit time effect, the gate voltage dependence of mobility and both drift and diffusion components. Velocity saturation effect is partially included in the NQS charge model by using the drain saturation voltage V_{DSAT} computed from the level-2 DC model. A new time step control scheme for NQS components is implemented to keep the local truncation error within a reasonable bound.

Contents

I. Introduction

Since currently available MOSFET capacitance models in circuit simulations are based on the quasi-static assumption, they fail when the relative signal change is faster than the inverse of channel transit time. Also there is uncertainty in the channel charge partitioning scheme.

Due to these problems, there had been difficulties in simulating high-speed and high-frequency analog circuits, especially the charge injection problem of switched analog circuits and the frequency response of high-frequency amplifiers.

To solve these problems, a few NQS(non-quasi-static) models have been suggested [4,5,6]. Turchetti et. al [4] reported a NQS transient MOSFET model for an assumed channel charge density profile which is linear for the QS component and is symmetrical for the NQS component. But since the assumed channel charge profile is over simplified, the usefulness of the model [4] is limited. Bagheri et. al.[5] derived a NQS AC model. But, in [5], iterations are needed to find the surface potentials and also to solve the continuity equation. Also, the model in [5] cannot be directly used in the large signal transient analysis because it is based on the small signal AC analysis. We reported a NQS MOSFET model [6] which predicts the NQS behavior accurately both for the transient [7] and AC [1] analyses but does not conserve charge for the transient analysis. In this work, we derived a charge based NQS MOSFET model for the transient analysis, which guarantees the charge conservation.

Although there is a simple DC model, based on the charge sheet formulation and shown in [1], the NQS charge model has been combined with the SPICE level-2 DC model and has been implemented in SPICE3B.1 [3] as *level*=5 model. Hence, the new implementation matches exactly the level-2 model in DC characteristics, and it recognizes all the level-2 model parameters. This strategy has been chosen because the SPICE level-2 model includes all the secondary effects, such as short and narrow channel effects on the bulk charge component, subthreshold conduction, velocity saturation, channel length modulation and temperature dependence. Another reason is that SPICE level-2 model parameters are widely available and it makes the new model easy to use.

And the drain saturation voltage V_{DSSAT} computed from the SPICE Level-2 DC model is used for the NQS charge model also. In this way, all the short channel effects, such as the velocity saturation effect, the V_{GS} dependence of mobility and all other aspects considered by the SPICE Level-2 model are also included in the charge model for transient and AC analyses. It is true that, while the DC model includes all the short channel effects, the charge model is still based on the long channel theory although short channel effects are partially included in the charge model through V_{DSSAT}. This compromise should be judged in the light of the fact that all the conventional charge (capacitance) models in SPICE (Meyer, Ward-Dutton, BSIM) don't

include any short channel effects either.

New time step control scheme has been implemented for the NQS charge component based on the local truncation error. It works fine for all the circuits tested.

The implementation details and simulation results of the simple DC model combined with the non-quasi-static charge model have been shown in the other work [1].

II. Model parameters

All the SPICE Level-2 model parameters except XQC (channel charge partitioning ratio) are recognized in this implementation. Model parameters of this implementation (level=5 model) are as follows. Almost all the parameters are described in [3] but they are repeated here for clarity.

Name	Meaning	Default	Unit
VTO (VT0)	threshold voltage at V_{BS}=0	0.0	V
KP	$W/L \cdot C_{OX} \cdot \mu$ at $V_{GS}=V_{TH}$	$2 \cdot 10^{-5}$	A/V^2
GAMMA	$\sqrt{2\varepsilon_{si} q N_{SUB}}/C_{OX}$	0.0	$\sqrt{V}$
PHI	$2\Phi_F = 2V_t \cdot \ln(N_{SUB}/n_i)$	0.6	V
LAMBDA	channel length modulation factor	0.0	V^{-1}
RD	drain series resistance	0.0	Ω
RS	source series resistance	0.0	Ω
CBD	B-D junction cap. at V_{BD}=0	0.0	F
CBS	B-S junction cap. at V_{BS}=0	0.0	F
IS	S,D junction saturation current	10^{-14}	A
PB	S,D junction potential	0.8	V
CGSO	G-S overlap capacitance / W	0.0	F/m
CGDO	G-D overlap capacitance / W	0.0	F/m
CGBO	G-B overlap capacitance / L	0.0	F/m
RSH	S,D junction sheet resistance	0.0	$\Omega/square$
CJ	unit area S,D junction cap.	0.0	F/m^2
MJ	S,D jct. bottom grading coeff.	0.5	-
CJSW	unit length jct. sidewall cap.	0.0	F/m
MJSW	junction sidewall grading coeff.	0.33	-
JS	unit area jct. sat. current	0.0	A/m^2
TOX	gate oxide thickness	10^{-7}	m

NSUB	bulk doping concentration	0.0	cm^{-3}
NSS	slow surface state density for computing V_{TH}	0.0	cm^{-2}
NFS	fast surface state density for subthreshold conduction	0.0	cm^{-2}
TPG	type of gate material for computing V_{TH} +1: opposite to bulk -1: same as bulk 0: Al	1.0	-
XJ	S,D junction depth, flag for short channel jct. effect	0.0	m
LD	S,D lateral diffusion	0.0	m
UO (U0)	surface mobility at $V_{GS}=V_{TH}$	600	$cm^2/V-s$
UCRIT	critical E-field for V_{GS} dependence of mobility	10^4	V/cm
UEXP	exponent for V_{GS} dependence of mobility	0.0	-
UTRA	V_{DS} effect on V_{GS} dependence of mobility, not used inside SPICE	0.0	-
VMAX	maximum drift velocity for computing velocity saturation effect	0.0	m/s
NEFF	multiplication factor for NSUB for computing channel length modulation with velocity saturation effect	1.0	-
FC	forward bias S,D jct. cap. coeff.	0.5	-
DELTA	narrow width effect on V_{TH}	0.0	-
QTRTOL	tolerance parameter for LTE, used in time step control	30.0	-
MINTOL	tolerance parameter for LTE, used in time step control	1.0	V
SATF	saturation factor for charge sheet formulation, factor A in eq.(2.15)	80	-

QTRTOL and MINTOL are tolerance parameters for the time step control. SATF is the

saturation factor A of the saturation function which determines the smoothness of the transition between linear and saturation regions. The saturation function is used to find the surface potential Ψ_{SL}, the surface potential at the drain end of the channel. All the parameters except QTRTOL, MINTOL, and SATF are the same as the SPICE Level-2 model parameters [3].

III. Model Equations

(a) DC analysis

For DC analysis, the same equations as level-2 model equations are used.[2,3]

(b) Transient analysis

From the current continuity equation, we can derive analytic equations for drain and source currents, and also for drain and source charges. The detailed derivation steps are shown in [1]. Hence, the drain, source, and gate currents, $I_D(t)$, $I_S(t)$, $I_G(t)$ can be written as

$$I_D(t) = I_{DC}(t) + \frac{dQ_D(t)}{dt} \tag{1.a}$$

$$I_S(t) = -I_{DC}(t) + \frac{dQ_S(t)}{dt} \tag{1.b}$$

$$I_G(t) = \frac{dQ_G(t)}{dt} \tag{1.c}$$

$$I_B(t) = -(I_D(t) + I_S(t) + I_G(t)) \tag{1.d}$$

$$Q_D(t) = -WC_{OX}\cdot\int_0^L \frac{y}{L}\cdot Q'_n(y,t)\,dy \tag{2.a}$$

$$Q_S(t) = -WC_{OX}\cdot\int_0^L (1-\frac{y}{L})\cdot Q'_n(y,t)\,dy \tag{2.b}$$

$$Q_G(t) = WC_{OX}\cdot\int_0^L V_{GB}(t)-V_{FB}-\Psi_{SO}(t)-\frac{V_{GST}(t)}{F_B}+\frac{Q'_n(y,t)}{F_B}\,dy \tag{2.c}$$

$$\textit{where}\quad V_{GST}(t) = V_{GB}(t) - V_{FB} - \Psi_{SO}(t) - \gamma\sqrt{\Psi_{SO}(t) - V_t} \tag{2.d}$$

$$F_B = 1 + \frac{0.5\gamma}{\sqrt{\Psi_{SO}(t)-V_t}}\left\{1 - \frac{1}{1.744+0.8364(\Psi_{SO}(t)-V_t)}\right\} \tag{2.e}$$

where $Q'_n(y,t)$ is the inversion charge density normalized by $(-WC_{OX})$, $Q_D(t)$, $Q_S(t)$, and $Q_G(t)$ are drain, source, and gate charges respectively. y is the lateral dimension along the channel from source (y=0) toward drain (y=L). Ψ_{SO} is the surface potential at the source end of the channel referenced to bulk [1], γ is the bulk effect coefficient $(\sqrt{2\varepsilon_{si}qN_{SUB}}/C_{OX})$, W is

the channel width, C_{OX} is the gate oxide capacitance per unit area, and V_t is the thermal voltage kT/q.

The DC current $I_{DC}(t)$ is computed using the SPICE level-2 DC model [2]. The normalized inversion charge density $Q'_n(y,t)$ can be represented as a sum of QS components (square root term and $F_B V_t$ term) and the NQS components (Fourier sine series term) [1], as.

$$Q'_n(y,t) = \sqrt{P_S(t) - (P_S(t) - P_D(t))\cdot\frac{y}{L}} - F_B V_t + \sum_{n=1}^{10} A_n(t)\cdot\sin(n\pi\cdot\frac{y}{L}) \tag{3.a}$$

where $$P_S(t) = (Q'_n(0,t) + F_B V_t)^2 \tag{3.b}$$

$$P_D(t) = (Q'_n(L,t) + F_B V_t)^2 \tag{3.c}$$

$$Q'_n(0,t) = V_{GST}(t) \tag{3.d}$$

$$Q'_n(L,t) = V_{GST}(t) - F_B\cdot(\Psi_{SL}(t) - \Psi_{SO}(t)) \tag{3.e}$$

Substituting the equation for $Q'_n(y,t)$ (3.a) into (2.a) and (2.b), one can get

$$Q_D(t) = -WLC_{OX}\cdot \left[\sqrt{P_S(t)}\cdot(\frac{2}{3}\cdot\frac{1-(1-a)^{1.5}}{a^2} - \frac{2}{5}\cdot\frac{1-(1-a)^{2.5}}{a^2}) - \frac{F_B V_t}{2} + \sum_{n=1}^{10}(-1)^{(n-1)}\cdot\frac{A_n(t)}{n\pi}\right] \tag{4.a}$$

$$Q_S(t) = -WLC_{OX}\cdot \left[\sqrt{P_S(t)}\cdot(-\frac{2}{3}\cdot(1-a)\cdot\frac{1-(1-a)^{1.5}}{a^2} + \frac{2}{5}\cdot\frac{1-(1-a)^{2.5}}{a^2}) - \frac{F_B V_t}{2} + \sum_{n=1}^{10}\frac{A_n(t)}{n\pi}\right] \tag{4.b}$$

where $$a(t) = 1 - \frac{P_D(t)}{P_S(t)} \tag{4.c}$$

the argument (t) in $a(t)$ is not shown in (4.a) and (4.b) for clarity. Since $a(t)$ comes in the denominator of (4.a) and (4.b), (4.a) and (4.b) are converted into asymptotic forms for small $a(t)$ ($a(t) < 10^{-3}$). Hence

$$Q_D(t) = -WLC_{OX}\cdot\left[0.5\sqrt{P_S(t)}\cdot(1-a\cdot(\frac{1}{3} + \frac{a}{16})) + \sum_{n=1}^{10}(-1)^{(n-1)}\cdot\frac{A_n(t)}{n\pi}\right] \tag{4.d}$$

$$Q_S(t) = -WLC_{OX}\cdot\left[0.5\sqrt{P_S(t)}\cdot(1-a\cdot(\frac{1}{6} + \frac{a}{48})) + \sum_{n=1}^{10}\frac{A_n(t)}{n\pi}\right] \tag{4.e}$$

(for $a(t) \le 10^{-3}$)

Substituting (2.a) and (2.b) into (2.c), one can represent $Q_G(t)$ in terms of $Q_D(t)$ and $Q_S(t)$.

$$Q_G(t) = WLC_{OX}\cdot\left[V_{GB}(t) - V_{FB} - \Psi_{SO}(t) - \frac{V_{GST}(t)}{F_B}\right] - \frac{Q_D(t) + Q_S(t)}{F_B} \tag{4.f}$$

Hence, once the coefficients $\{A_n(t)\}$ are computed, one can get all the values of node currents and node charges.

Substituting (3.a) into the current continuity equation, one can get the state equation for the coefficients $\{A_n(t)\}$ [1].

$$\frac{d\mathbf{B}}{dt} = \mathbf{D} \cdot \mathbf{B} + \mathbf{G_S} \cdot \frac{dP_S}{dt} + \mathbf{G_D} \cdot \frac{dP_D}{dt} \tag{5}$$

where **B** is a column matrix for the coefficients $\{B_n\}$, **B** is a tri-diagonal square matrix, and $\mathbf{G_S}$ and $\mathbf{G_D}$ are column matrices. The column matrix **B** is derived from the column matrix **A** whose coefficients are $\{A_n\}$ in (3.a). Hence, coefficients $\{B_n\}$ are used only inside the model computation routine and coefficients $\{A_n\}$ are used outside of the model computation routine.

$$B_n = A_n \qquad (for\ n=1,3,5,7,9) \tag{6.a}$$

$$= (xnrm - xrev)\cdot A_n \qquad (for\ n=2,4,6,8,10)$$

where *xnrm* and *xrev* are the indicators about whether V_{DS} is positive or not.

$$xnrm = 1 \qquad (for\ V_{DS} \geq 0) \tag{6.b}$$

$$= 0 \qquad (for\ V_{DS} < 0)$$

$$xrev = 0 \qquad (for\ V_{DS} \geq 0) \tag{6.c}$$

$$= 1 \qquad (for\ V_{DS} < 0)$$

where V_{DS} is the applied drain-to-source voltage and *D* and *S* refer to drain and source as specified in SPICE input, that is, *D* and *S* in

Mx D G S B model_name w=x l=x ad=x as=x pd=x ps=x

Coefficients of the tri-diagonal square matrix **D** are computed from

$$D_{i,(i-1)} = -\frac{\mu_n}{2F_B}\cdot\frac{\pi^2}{L^2}\cdot i^2 \cdot D1 \tag{7.a}$$

$$D_{i,i} = -\frac{\mu_n}{2F_B}\cdot\frac{\pi^2}{L^2}\cdot i^2 \cdot D0 \tag{7.b}$$

$$D_{i,(i+1)} = -\frac{\mu_n}{2F_B}\cdot\frac{\pi^2}{L^2}\cdot i^2 \cdot D1 \tag{7.c}$$

(for i=1,2,3,...,10, but $D_{1,0} = D_{10,11} = 0$)

$$D0 = \frac{4}{3}\cdot\sqrt{P_S}\cdot\frac{1-(1-a)^{1.5}}{a} + \frac{2}{\pi}\cdot\sum_{m=1}^{5}\frac{B^{(old)}_{2m-1}}{2m-1} \tag{8.a}$$

$$= 2\sqrt{P_S}\cdot(1-\frac{a}{4}) + \frac{2}{\pi}\cdot\sum_{m=1}^{5}\frac{B^{(old)}{}_{2m-1}}{2m-1} \qquad (for\ a < 10^{-5})$$

where $\{B^{(old)}{}_{2m-1}\}$ are $\{B_{2m-1}\}$ at the previous time point. $a^{0.25}$ is added to set $D1$ to 0, when a=0, that is, when cutoff or when V_{DS}=0.

$$D1 = (\sqrt{P_S} - \frac{D0}{2})\cdot a^{0.25} \tag{8.b}$$

The coefficients of the column matrices $\mathbf{G_S}$ and $\mathbf{G_D}$ are computed from

$$G_{S.2m} = -\frac{(1-\frac{a}{2})\cdot C1 + (b + 2(1-a)\cdot\frac{db}{da})\cdot C2}{2m\pi\sqrt{P_S}} \tag{9.a}$$

$$G_{S.2m-1} = -\frac{(1+\frac{a}{2})\cdot C1 - (b+2(1-a)\cdot\frac{db}{da})\cdot(1-\frac{4}{\pi^2(2m-1)^2})\cdot C2}{(2m-1)\pi\cdot\sqrt{P_S}} \tag{9.b}$$

$$G_{D.2m} = \frac{C1\cdot(1+2\frac{db}{da})}{2m\pi\cdot\sqrt{P_S}} \tag{9.c}$$

$$G_{D.2m-1} = -\frac{C1 + 2\cdot\frac{db}{da}\cdot(1-\frac{4}{\pi^2(2m-1)^2})\cdot C2}{(2m-1)\pi\cdot\sqrt{P_S}} \tag{9.d}$$

(for m = 1, 2, 3, 4, 5)

where

$$b = 3 - \frac{3}{4}a - \frac{2}{a}\cdot(1-(1-a)^{1.5}) \tag{9.e}$$

$$= \frac{a^2}{8} \qquad (\text{for } a < 10^{-4})$$

db/da is the derivative of b with respect to a. $C1$ and $C2$ are constants to compensate for the truncation error, that is, the error due to the truncation of the Fourier series in (3.a) into 10 terms, where C1 = 1.0420956770489359 and C2 = 1.0644098681085510.

By appling the trapezoidal integration scheme to (5), one can compute the partial derivatives of **B** as follows.

$$(\mathbf{I} - \frac{\mathbf{k}}{2}\mathbf{D})\cdot\frac{\partial\mathbf{B}}{\partial t} = \mathbf{D}\cdot\mathbf{B}^{(old)} \tag{10.a}$$

$$(\mathbf{I} - \frac{\mathbf{k}}{2}\mathbf{D})\cdot\frac{\partial\mathbf{B}}{\partial P_S} = \mathbf{G_S} \tag{10.b}$$

$$(\mathbf{I} - \frac{\mathbf{k}}{2}\mathbf{D})\cdot\frac{\partial\mathbf{B}}{\partial P_D} = \mathbf{G_D} \tag{10.c}$$

where k is the time step, and $\mathbf{B}^{(old)}$ is the column matrix of coefficients $\{B_n\}$ computed at the previous time point. Values at the previous time point are used for column matrices $\mathbf{D}$, $\mathbf{G_D}$, and $\mathbf{G_S}$ in (10.a), (10.b) and (10.c). The new $\mathbf{B}$ at the present time point can be computed from the partial derivatives of $\mathbf{B}$ in (10.a), (10.b), and (10.c).

$$\mathbf{B} = \mathbf{B}^{(old)} + \frac{\partial \mathbf{B}}{\partial t}\cdot k + \frac{\partial \mathbf{B}}{\partial P_S}\cdot \Delta P_S + \frac{\partial \mathbf{B}}{\partial P_D}\cdot \Delta P_D \tag{11}$$

ΔP_S and ΔP_D are changes of P_S and P_D respectively during the present time step, that is, the time interval $[t-k, t]$, where t is the present time point.

The derivatives of $\mathbf{B}$ which are used in computing the derivatives of node currents with respect to applied biases can be computed from

$$\frac{\partial \mathbf{B}}{\partial V_X} = \frac{\partial \mathbf{B}}{\partial P_S}\cdot\frac{\partial P_S}{\partial V_X} + \frac{\partial \mathbf{B}}{\partial P_D}\cdot\frac{\partial P_D}{\partial V_X} \tag{12}$$

$$(\text{where } V_X = V_G, V_D, V_S, V_B)$$

The moving-boundary condition [1] is not used in this implementation for simplicity.

(c) AC analysis

Since the charge conservation is not a problem for the AC analysis, the AC model doesn't have to be a charge-based model. Hence, analytic equations are derived for node currents for the AC model equations [1]. The NQS AC model has been implemented such that it matches the level-2 model in DC characteristics.

For the small-signal sinusoidal excitation, we decompose $P(y,t)$ into the DC components and the small-signal component [1], where $P(y,t) = (Q_n'(y,t) + F_B V_t)^2$.

$$P(y,t) = P_S\cdot\left(1-\left(1-r\right)\cdot\frac{y}{L}\right) + p(y,\omega)\cdot e^{j\omega t} \tag{13.a}$$

$$\textit{where}\quad r = 1 - \frac{P_D}{P_S} \tag{13.b}$$

where P_S and P_D are DC values at the DC operating point and $p(y,\omega)$ is the phasor of the sinusoidal excitation. r in (13.b) is essentially the same as $a(t)$ in (4.c), but r is a DC quantity while $a(t)$ is a time varying quantity. Substituting (13.a) into the diffusion equation which has been derived from the current continuity equation and the current relation [1,6], one can get

$$\alpha^2\cdot p(y',\omega) = \frac{\partial^2 p(y',\omega)}{\partial y'^2}\cdot\sqrt{1-r\cdot y'} \tag{14.a}$$

$$\textit{where}\ \ \alpha = \sqrt{j\,\frac{\omega}{\omega_T}} = (1+j)\cdot\sqrt{\frac{\omega}{2\omega_T}} \tag{14.b}$$

$$\omega_T = \frac{\mu_n (V_{GST}+F_B V_t)}{F_B L^2} = \frac{1}{\tau_T} \tag{14.c}$$

where $y' = y/L$ and τ_T is the channel transit time. ω_T is determined by the DC operating point using the SPICE level-2 DC model.

If r=0, the exact solution to (14.a) is $e^{\alpha y'}$ and $e^{-\alpha y'}$. Observing that the factor r lies between 0 and 1, we approximate the solution to (14.a), including the perturbation by non zero r, as

$$p(y',\omega) = G\cdot e^{\alpha y'}\cdot(1+b_1 y'+b_2 y'^2) + H\cdot e^{-\alpha y'}\cdot(1+d_1 y'+d_2 y'^2) \tag{15}$$

Eq. (15) is different from the early version of this work briefly described in [6] and y'^2 terms are newly added for good approximation. The coefficients b_1,b_2,d_1 and d_2 are asymmetry factors and can be found by substituting (15) into (14.a) and matching $p(0,\omega)$ and the integrated $p(y',\omega)$ from y'=0 to y'=1, in both sides of the equation. Hence,

$$b_1 = \frac{-B}{C - E\cdot\alpha} \tag{16.a}$$

$$b_2 = -\alpha\cdot b_1 \tag{16.b}$$

$$d_1 = \frac{-B}{C + E\cdot\alpha} \tag{16.c}$$

$$d_2 = \alpha\cdot d_1 \tag{16.d}$$

$$B = r^2\left\{ r-\frac{2}{3}(1-(1-r)^{1.5})\right\} \tag{16.e}$$

$$C = 3r\left\{\frac{2}{3}(1-(1-r)^{1.5}) - \frac{2}{5}(1-(1-r)^{2.5})\right\} + 0.5r^3 \tag{16.f}$$

$$E = \frac{r^3}{3} - \frac{2}{3}(1-(1-r)^{1.5}) + \frac{4}{5}(1-(1-r)^{2.5}) - \frac{2}{7}(1-(1-r)^{3.5}) \tag{16.g}$$

Coefficients B,C and E are real positive numbers which increase monotonically with r.

From the two boundary values of $p(y',\omega)$ at the source and the drain ends, p_S and p_D, we can find the coefficients G and H.

$$G = \frac{p_S(1+d_1+d_2)\cdot e^{-\alpha} - p_D}{(1+d_1+d_2)\cdot e^{-\alpha} - (1+b_1+b_2)\cdot e^{\alpha}} \tag{17.a}$$

$$H = \frac{p_D - p_S(1+b_1+b_2)\cdot e^{\alpha}}{(1+d_1+d_2)\cdot e^{-\alpha} - (1+b_1+b_2)\cdot e^{\alpha}} \tag{17.b}$$

The phasors p_S and p_D can be found using the derivatives of P_D and P_S in (3.b) and (3.c)

with respect to applied biases.

$$p_S = \frac{\partial P_S}{\partial v_G}\cdot v_G + \frac{\partial P_S}{\partial v_B}\cdot v_B + \frac{\partial P_S}{\partial v_D}\cdot v_D + \frac{\partial P_S}{\partial v_S}\cdot v_S \tag{18.a}$$

$$p_D = \frac{\partial P_D}{\partial v_G}\cdot v_G + \frac{\partial P_D}{\partial v_B}\cdot v_B + \frac{\partial P_D}{\partial v_D}\cdot v_D + \frac{\partial P_D}{\partial v_S}\cdot v_S \tag{18.b}$$

where v_G, v_B, v_D and v_S are the small-signal phasors of each node voltage respectively. Eq. (18.a) and (18.b) are based on the assumption that the small-signal excitations at source and drain ends follow the applied biases instantaneously.

The small-signal channel current i_y can be written as [1]

$$i_y(y',\omega) = \beta_p \cdot \frac{\partial p(y',\omega)}{\partial y'} \tag{19.a}$$

$$\textit{where} \qquad \beta_p = \frac{W}{L}\cdot C_{OX}\cdot\frac{\mu_n}{2F_B}\cdot F_{CLM} \tag{19.b}$$

where F_{CLM} is the channel length modulation factor which is computed using the SPICE level-2 DC model [2]. From (15) -(17), and (19), the small-signal drain and source currents can be written as

$$i_D = \beta_p \tag{20.a}$$

$$\frac{p_S\cdot\left[((C^2-BE)-(B-E)^2\cdot\alpha^2)\cdot\alpha\right] - p_D\cdot\left[(-BC+B(3E-C)\cdot\alpha^2)\cdot\sinh\alpha + (C^2-BE+BC+E(B-E)\cdot\alpha^2)\cdot\alpha\cdot\cosh\alpha\right]}{(C(C-B)+E(B-E)\cdot\alpha^2)\cdot\sinh\alpha + B(C-E)\cdot\alpha\cdot\cosh\alpha}$$

$$i_S = -\beta_p \tag{20.b}$$

$$\frac{p_S\cdot\left[(B(C-B)+B(C-E)\cdot\alpha^2)\cdot\sinh\alpha + (B(B-E)+C(C-B)+E(B-E)\cdot\alpha^2)\cdot\alpha\cdot\cosh\alpha\right] - p_D\cdot\left[(C^2-BE-E^2\cdot\alpha^2)\cdot\alpha\right]}{(C(C-B)+E(B-E)\cdot\alpha^2)\cdot\sinh\alpha + B(C-E)\cdot\alpha\cdot\cosh\alpha}$$

From (18) and (20), one can find the derivatives of i_D and i_S with respect to applied biases.

Small signal bulk current i_B can be derived from the quasi-static bulk capacitances [1,8].

$$i_B = j\omega\cdot(C_{BG}\cdot v_G + C_{BB}\cdot v_B + C_{BD}\cdot v_D + C_{BS}\cdot v_S) \tag{21.a}$$

AC gate current i_G can be computed from the other three current components.

$$i_G = -(i_D + i_S + i_B) \tag{21.b}$$

IV. Time step control

To get the accuracy and the reasonable CPU time for the transient analysis, we need a time step control scheme. Two kinds of state equations are solved in this work.

One type of the state equation is (22) for the currents through the overlap and junction capacitances.

$$I = \frac{dQ}{dt} \tag{22}$$

The original time step control scheme in SPICE [9] is used for this type of state equation.

The other type of state equation is shown in eq. (5). To solve (5), the values at the previous time point (t_0) are used for the matrices $\mathbf{D}$, $\mathbf{G_S}$, and $\mathbf{G_D}$. Using the trapezoidal integration, the local truncation error LTE can be written as

$$\begin{aligned} LTE &= norm\left(\Delta\mathbf{A}\,|_{(exact)} - \Delta\mathbf{A}\,|_{(approx)}\right) \\ &= \frac{k^2}{2}\cdot norm\left[\mathbf{D}'(t_0)\cdot\mathbf{A}(t_0) + \mathbf{G_S}'(t_0)\cdot\mathbf{P_S}'(t_0) + \mathbf{G_D}'(t_0)\cdot\mathbf{P_D}'(t_0)\right] \end{aligned} \tag{23.a}$$

Since A_1 is dominant over other coefficients of $\{A_n\}$ for n = 2, 3, ..., 10, under most of operating conditions, only A_1 is considered in the time step control for simplicity. Hence,

$$LTE = \frac{k^2}{2}\cdot\left|\frac{dD_{11}}{dt}\cdot A_1 + \frac{dD_{12}}{dt}\cdot A_2 + \frac{dG_{S.1}}{dt}\cdot\frac{dP_S}{dt} + \frac{dG_{D.1}}{dt}\cdot\frac{dP_D}{dt}\right| \tag{23.b}$$

The time derivatives in (23.b) are computed using the divided difference method. The LTE in (23.b) must be less than the tolerance limit.

$$LTE \le QTRTOL\cdot\left(RELTOL\cdot\left(MINTOL + \max(A_1(t),A_1(t_0))\right)\right) \tag{24}$$

where t is the present time point and t_0 is the previous time point. *QTRTOL* and *MINTOL* can be specified in the model card.

V. Implementation in SPICE3B1

This NQS charge model combined with the Level-2 DC model has been implemented into SPICE3B.1 [3]. Compared to SPICE2 [10], SPICE3 is written so modularly that each model routine can be quite independent of other model routines with minimal changes in files outside of the model routine. Hence, it is much easier to add a new model into SPICE3 than into SPICE2. All the model routines for this work are placed in the directory

DEV/NQS

The files outside of the model routine which need changes are

DEV/Makefile
CKT/SIMinit.c

INP/INPpas2.c
INP/INPdomodel.c
INP/INPfindLev.c

In "DEV/Makefile", 'NQS' is added in the list of device models.

The file "SIMinit.c" contains the routine which initializes the data structure for the circuit to be simulated before starting the simulation. Two lines are inserted in "SIMinit.c" to add a new model. One is the following line in the variable declaration.

```
extern SPICEdev  NQSinfo;
```

The other is the following line in the lists of the data structure "SPICEdev *DEVices [ ]".

```
&NQSinfo
```

The file "INPpas2.c" contains the routine which processes SPICE3 input file, line by line, and checks whether the input is correctly specified or not. When the first character of the input line is 'M', the program switches to the part of the routine which checks the syntax of the MOSFET element, that is,

```
Mx D G S B model_type w=x l=x
```

The routine also checks whether the specified "model_type" is available in the program. Hence we add the following line in this part of the routine to let the routine know that the new model is available.

```
&&(thismodel->INPmodType != INPtypelook("NQS"))
```

The file "INPdomodel.c" contains the routine which identifies the model type and generates a data structure for the model. In the standard SPICE3B.1 release [3], four kinds of MOSFET models are available, that is, level-1(MOS1), level-2(MOS2), level-3(MOS3), and level-4(BSIM). To add this work as level-5 MOSFET model, we add the following three lines twice, once for 'nmos' and once for 'pmos'.

```
case 5:
        type = CKTtypelook("NQS");
```

```
break;
```

The file "INPfindLev.c" contains the routine which extracts the level of MOSFET models from the SPICE3 input line and returns the value of the level to the calling routine. To add this work as a level-5 model, we add the following three lines inside the switch block of the routine.

```
case '5':
    *level = 5;
    return((char *)NULL);
```

The *return* statement above is just a house keeping stuff.

The model is routine is decomposed into several files. Names of the files, the subroutines in the files, and their functions are as follows.

File	Subroutine	Function
NQSdefs.h	-	define data structures for MOSFET element and MOSFET model
NQS.c	-	define data structures for MOSFET element parameter table, model parameter table, and subroutines
NQSeval.c	NQSevaluate	model computation routine, computes node currents, node charges and their derivatives w.r.t. node voltages
NQSload.c	NQSload	process MOSFETs for DC and transient analysis, fill in Jacobian matrix and RHS vector by calling NQSevaluate. This routine is called once per iteration.
NQSacLoad.c	NQSacLoad	process MOSFETs for AC analysis
NQSpzLoad.c	NQSpzLoad	process MOSFETs for pole-zero analysis, not implemented yet
NQSsetup.c	NQSsetup	allocates memory for the sparse matrix elements for the given circuit
	NQSvsSetup	allocates memory for the cubic spline function and compute the cubic

		spline coefficients
	NQScubicSp	compute the cubic spline coefficients from a set of (x,y) data
NQStemp.c	NQStemp	default value processing for model parameters including the temperature effect
NQStrunc.c	NQStrunc	time step (LTE) control
NQSmosCap.c	NQSmosCap	process overlap capacitors for transient analysis
NQSparam.c	NQSparam	process SPICE3 input lines for MOSFET elements
NQSmParam.c	NQSmParam	process SPICE3 input lines for MOSFET models
NQSgetic.c	NQSgetic	grab initial condition
NQSdelete.c	NQSdelete	free the memory allocated to a data structure of MOSFET element
NQSmDelete.c	NQSmDelete	free the memory allocated to a data structure of MOSFET model
NQSdestroy.c	NQSdestroy	free the memory allocated to data structures of all MOSFET elements

VI. Simulation Results and Performance Comparison

Some circuits are simulated both with NQS model and Level-2 Meyer model. SPICE3 input files for Fig.2, 3, 4 and 5 are shown in the appendix.

(a) DC analysis

DC and AC analysis results of a folded cascode CMOS OP amp (Fig.1) are shown in Fig.2 and 3. In the DC analysis, this model gives exactly the same results as the Level-2 model as shown in Fig.2.

(b) AC analysis

In the AC analysis, this model gives quite different results from the Level-2 Meyer model especially in phase response as shown in Fig.3. Table 1 shows the comparison of the run statistics of some circuits for the AC analysis using the NQS and Level-2 Meyer model. For the AC analysis, the NQS model requires CPU time twice longer than the Level-2 Meyer model.

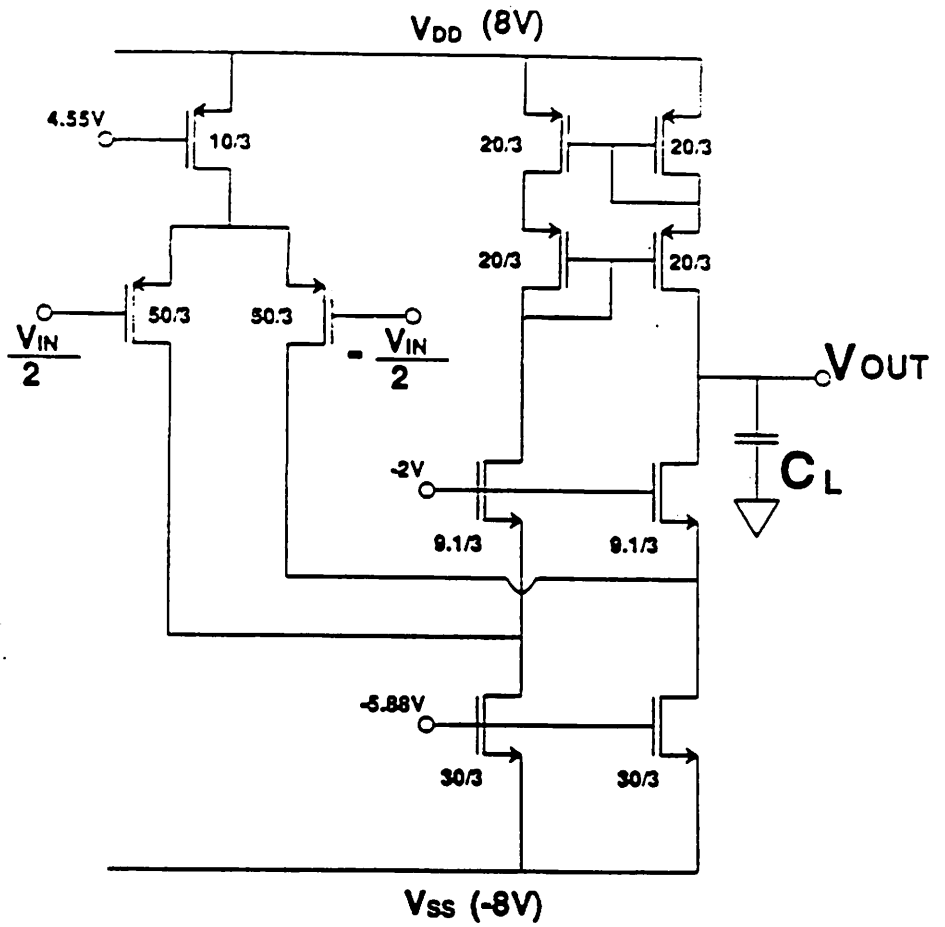

Fig.1 Circuit schematic of a folded cascode CMOS OP Amp [13]

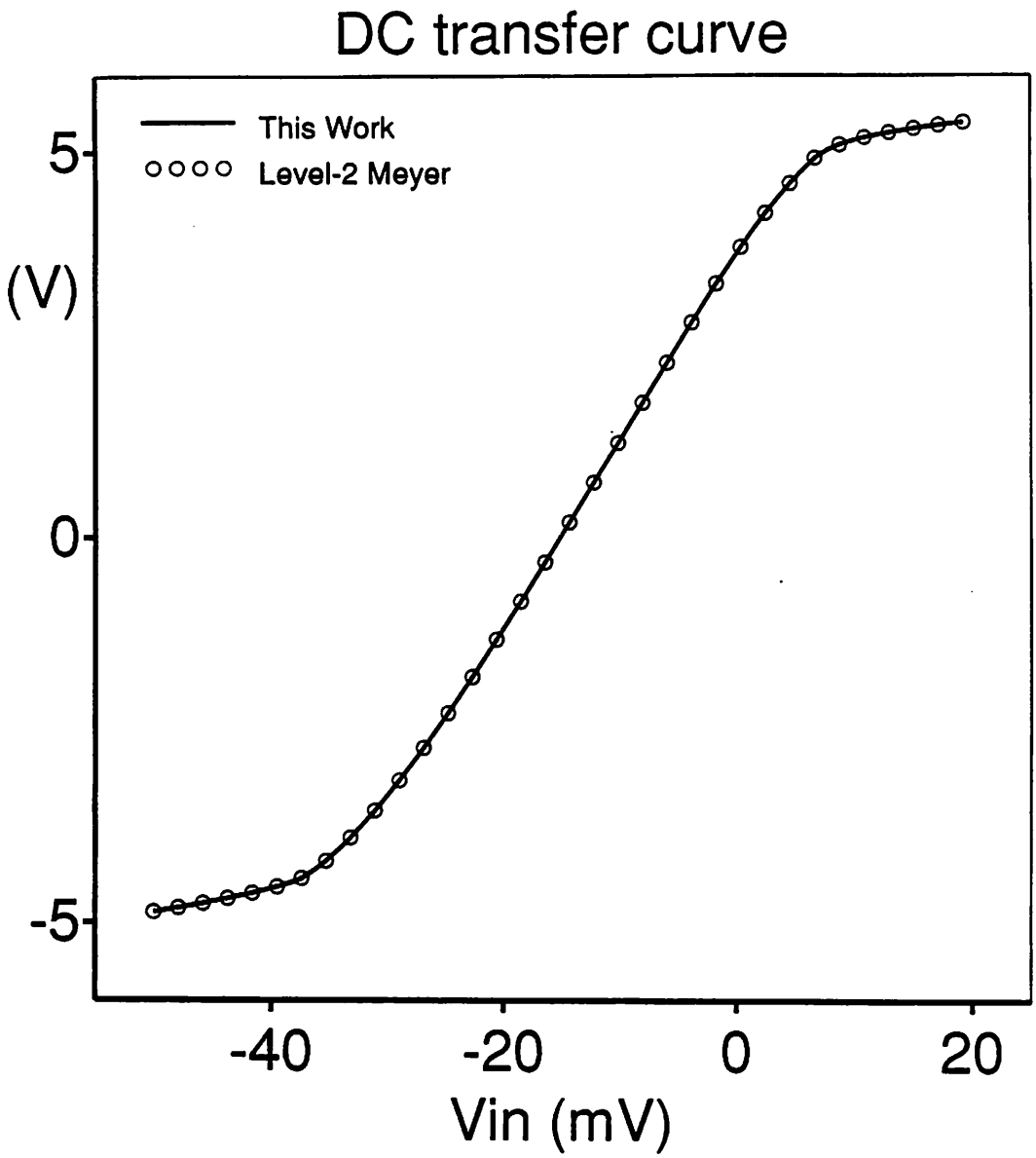

Fig.2 DC transfer curve of the folded cascode CMOS OP Amp in Fig.1.

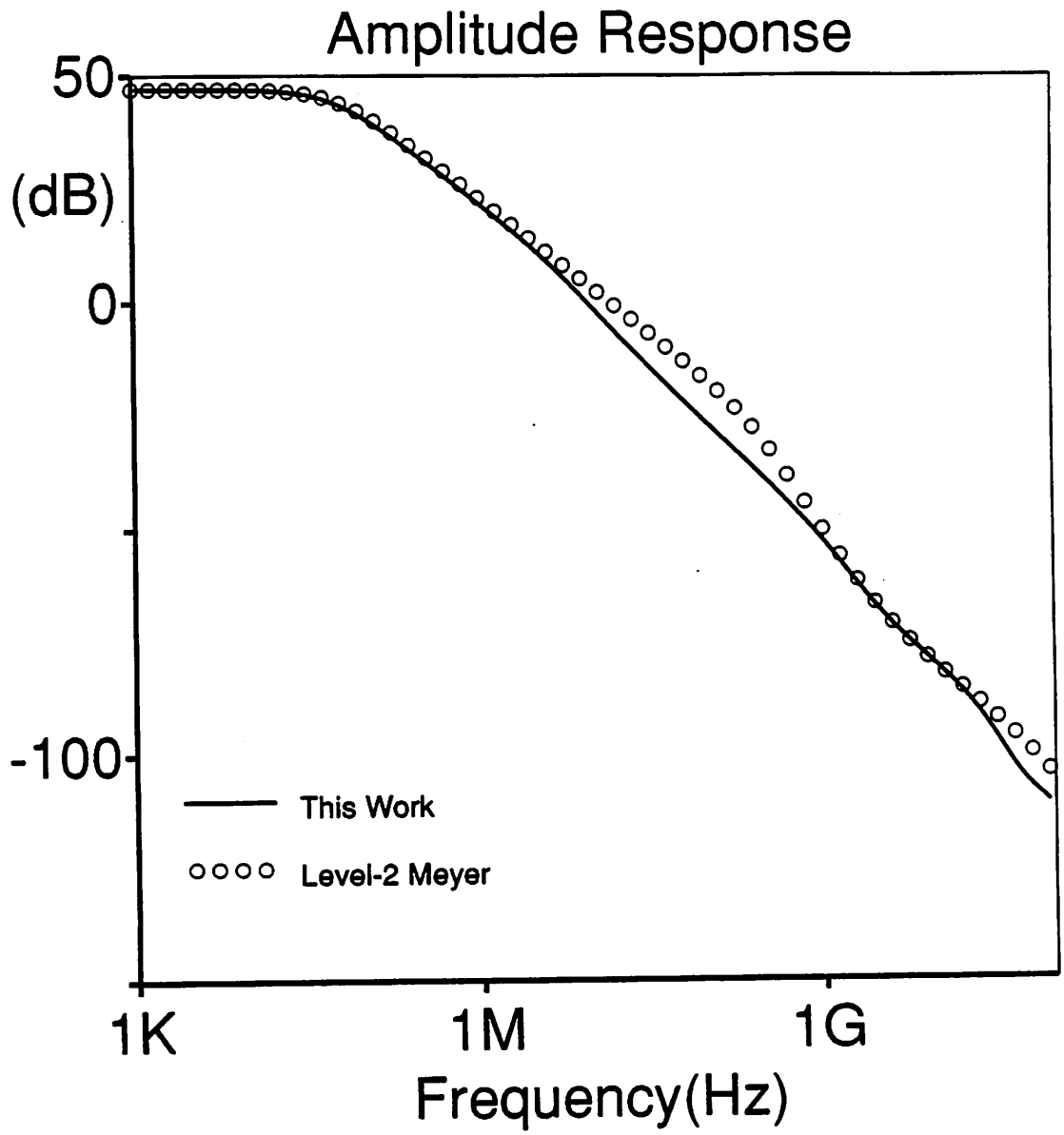

Fig.3.(a) Magnitude response of the folded cascode OP Amp in Fig.1.

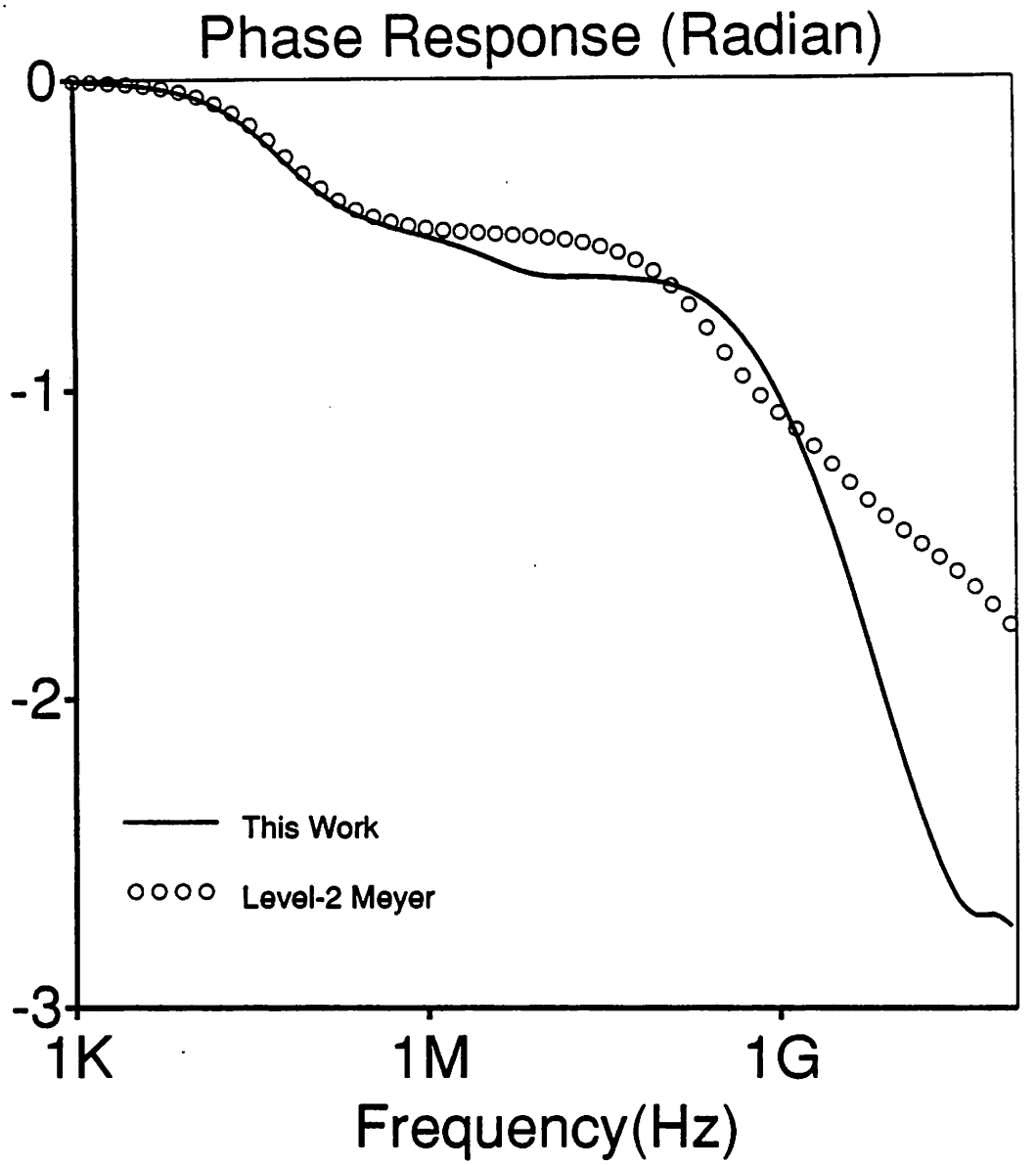

Fig.3.(b) Phase response of the folded cascode OP Amp. in F1g.1. The vertical unit is in π radian.

	cascode OP Amp
Total Run Time(sec)	5.5 (3.5)
Load Time (sec)	0.3 (0.14)

Table.1. Comparison of run statistics of the AC analysis of a folded cascode CMOS OP Amp. The quantities inside the parentheses represent the Level-2 Meyer model.(VAX 8800, Ultrix V-2.2)

(c) Transient analysis

The turn-off transient of a NMOSFET pass transistor has been simulated using this work, the SPICE level-2 charge based model [2], and the results are compared with those from a mixed mode simulator CODECS [11]. The magnitude of the output error voltage versus the fall time T_F is shown in Fig.4. The input voltage V_{IN} is set to DC 0 V. Although the polarity of V_{OUT} is negative due to the injection of channel charge into the capacitor (2pF) connected to the output node (node S), only the absolute values of the output error voltage are shown in Fig.4 for clarity.

For the slow turn-off (large T_F), the node S is connected to ground via a high impedance path (2pF capacitor), and the node D is connected to ground via a relatively low impedance path (10K resistor). Hence most of the channel charge is injected to the node D and very little channel charge is injected to the node S, and so all the models show the small output error voltage for the slow turn-off (large T_F) in Fig.4.

For the fast-turnoff where T_F is less than 20ns (RC time constant of 2pF capacitor and 10K resistor), the impedance between the node D and ground becomes comparable to that between the node S and ground. Hence half of the channel charge is injected to the node D, as shown by this work and CODECS in Fig.4. But the SPICE level-2 charge based model with XQC=0.0 gives the output error voltage which is much larger than that of this work, because the model with XQC=0.0 assigns most of the channel charge to the source node, that is, the node S (output node). For the SPICE level-2 charge based model with XQC=0.4999, about half of the channel charge is assigned to each of drain or source node. Hence this agrees with the above-mentioned physical phenomenon for the fast turn-off and it gives the good agreement with this work and CODECS. Therefore, XQC=0.4999 is the good partitioning scheme for this particular example. The comparison of run statistics for this example (Fig.4) is shown in Table 2.

Fig.5 shows the differential output error voltage of a differential sample-hold circuit[12], using this work and the SPICE level-2 Meyer model. The Meyer model gives more spurious spikes than this work.

Table 3 shows the comparison of the run time statistics for transient analyses of many example circuits, such as, a 2 stage CMOS OP Amp('2-stage')[13], a folded cascode CMOS OP Amp('cascode')[13], a differential sample-hold circuit ('diff.sh') [12], an 11-stage CMOS ring oscillator ('crosc'), an 11-stage E-D NMOS ring oscillator('drosc').

For the transient analysis, the CPU time of NQS model per iteration is about twice longer than that of Level-2 Meyer model. For the CMOS OP amps, the CPU time for NQS model is about four times longer than that for Level-2 Meyer model and for the ring oscillators, it is 15 times longer for the NQS model.

	This Work	Level-2 Meyer	Level-2, XQC=0.5	CODECS
CPU Time(sec)	2.3	1.1	1.2	1158
# of Iter.	423	173	169	304
Total Time Pts	151	77	76	116
Reject Time Pts	37	4	5	13
Load Time(sec)	1.5	0.5	0.6	1151

Table 2. Comparison of run statistics for the turn-off transient of an NMOS pass-transistor shown in Fig.4. (VAX 8800, Ultrix V-2.2)

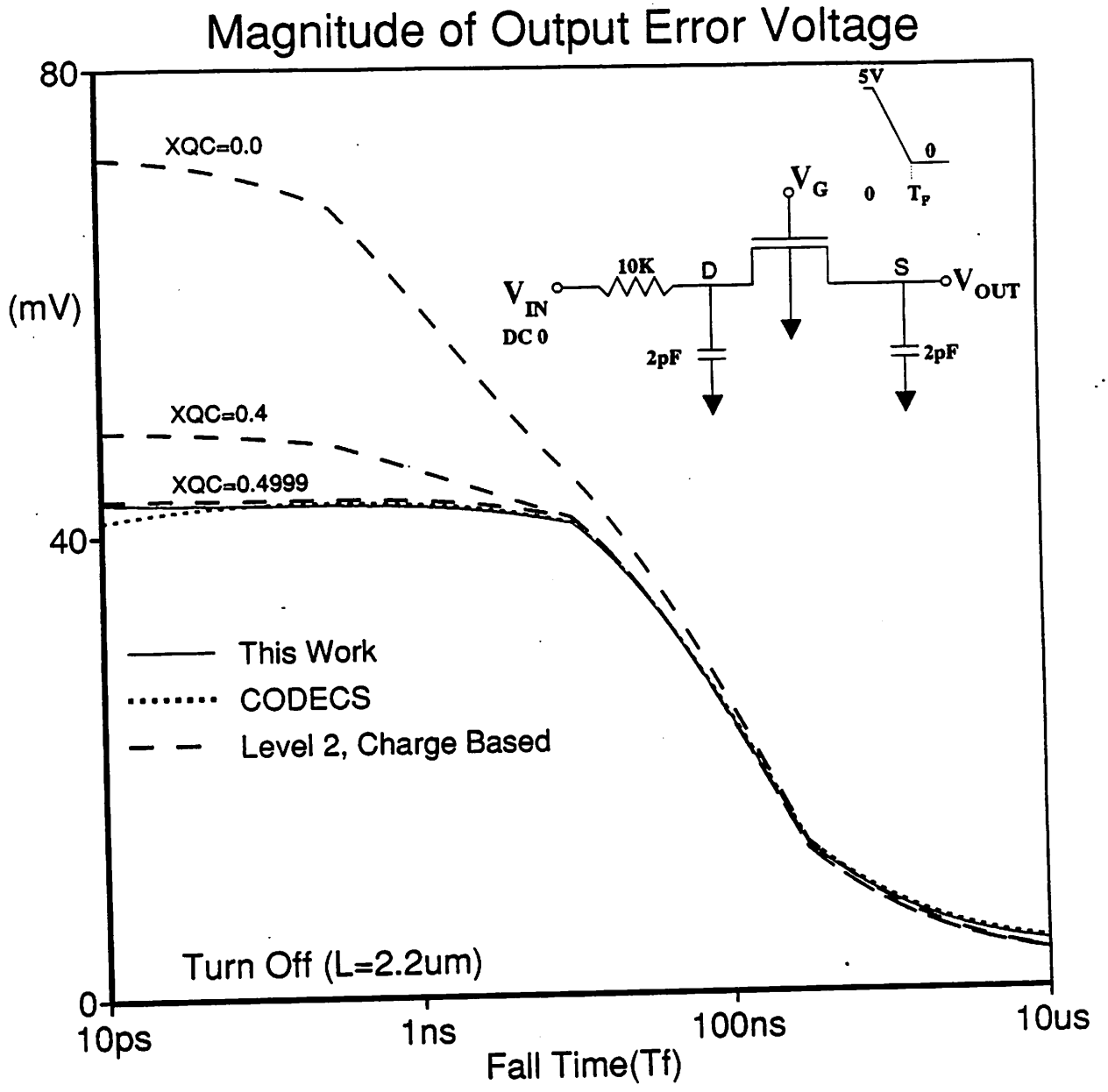

Fig.4. Comparison of this work(SPICE level-2 DC model + NQS charge model) with CODECS [11] and the SPICE level-2 charge-based model [2], for the output error voltages versus the fall time of the gate pulse, at the turn-off transient of a NMOS pass transistor. W/L of the NMOSFET is $20\mu m/3\mu m$ (drawn dimension) Model parameters used for this work and the SPICE level-2 charge based model are extracted from the DC current characteristics of the CODECS simulation.

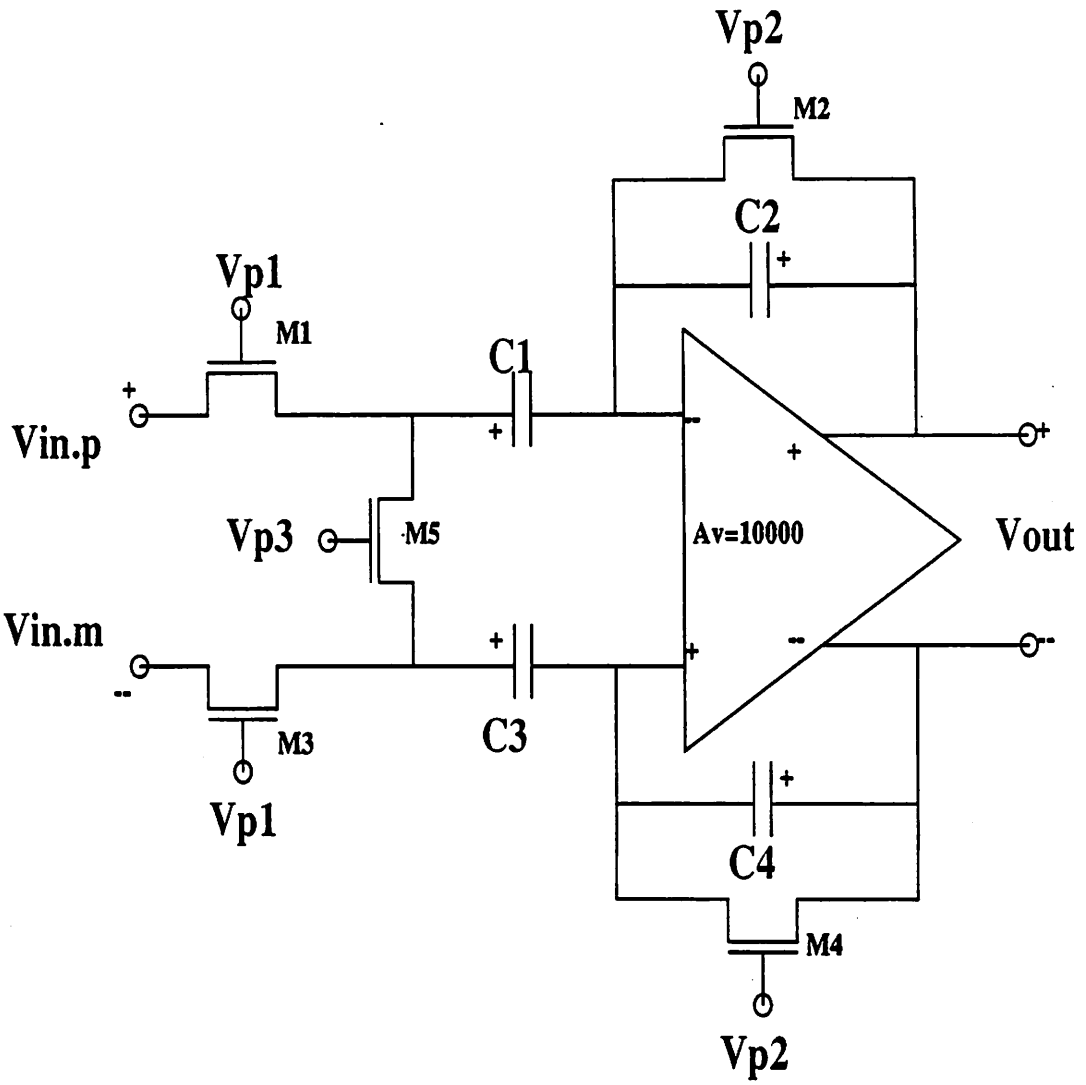

W/L (M1.M2,M3,M4)=200/3um

W/L (M5) = 20/3um

C1 = C2 = C3 = C4 = 1pF

Fig.5.(a) Circuit schematic of a differential sample-hold circuit [12].

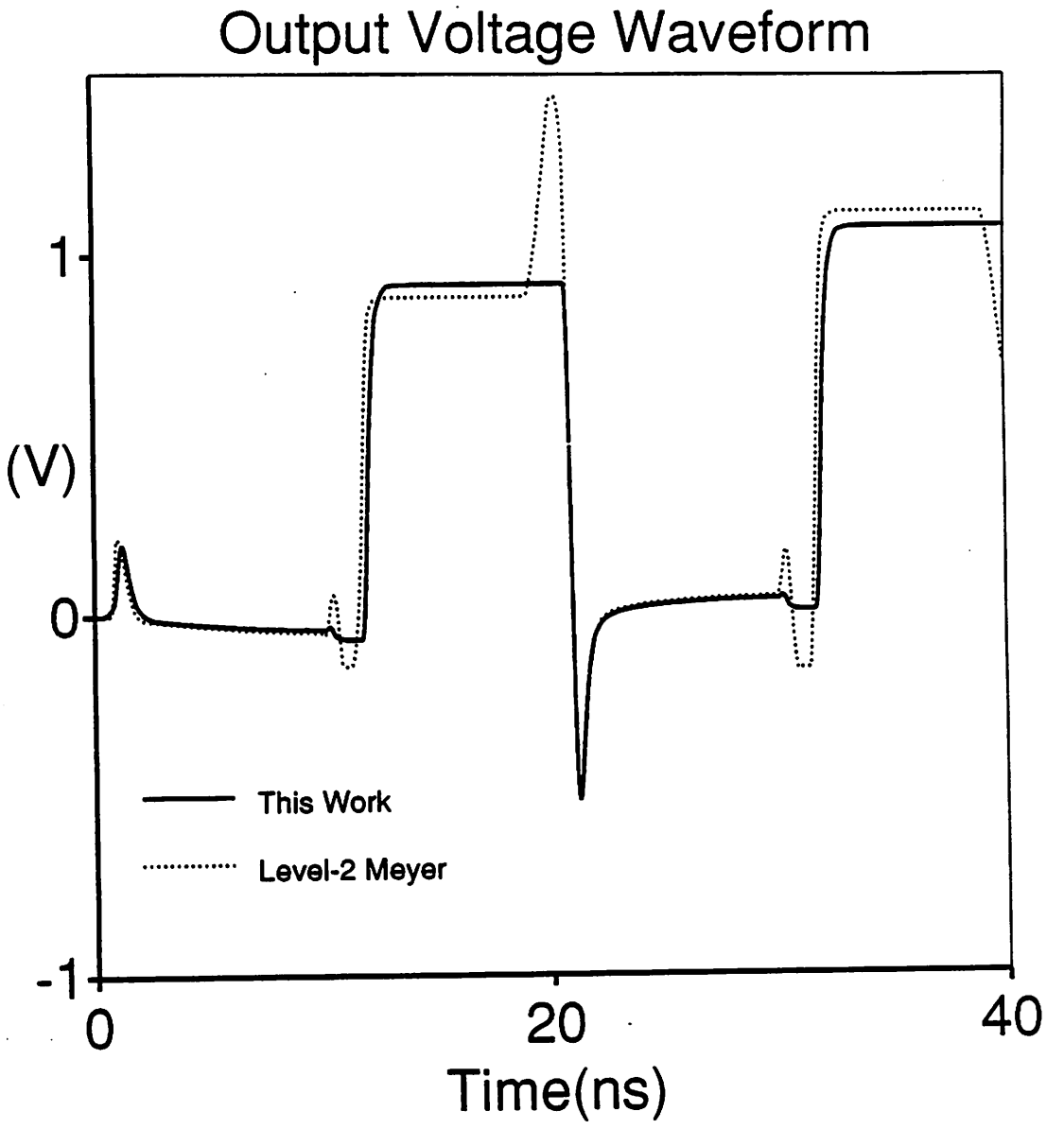

Fig.5.(b) Differential output voltage waveform of a differential sample-hold circuit.

	2-stage	cascode	diff.sh	crosc	drosc
Total CPU time(sec)	25 (6)	18(7.5)	43 (10)	1827 (123)	488 (28)
Total iter.	740 (342)	325 (247)	2000 (1008)	3925 (67)	6041 (1269)
Reject. Time Pts.	26 (13)	9 (7)	36 (60)	196 (67)	109 (101)
Load Time(sec)	22 (4.4)	15 (5.2)	37 (7)	1673 (94)	461 (24)

Table.3. Comparison of run statistics for the transient analyses using this work and the SPICE Level-2 Meyer model.(VAX 8800, Ultrix V-2.2)

Acknowledgements

This work has been supported by S.R.C., Intel and California State MICRO. One of the authors H.J.Park would like to express his special thanks to Professor P.R.Gray and D.O.Pederson for the suggestion of this implementation and also to graduate students T.L.Quarles and K.Mayaram for discussions.

References

[1] H.J.Park, "Charge-Sheet and Non-Quasistatic MOSFET Models for SPICE", Memorandum No. UCB/ERL M89/20, Electronics Research Lab., Dept. of EECS, University of California, Berkeley, 24 Feb. 1989

[2] A.Vladimirescu, S.Liu, "The Simulation of MOS Integrated Circuits using SPICE2", ERL Memo, M80/7, U.C.Berkeley, Oct., 1980

[3] T.L.Quarles, A.R.Newton, D.O.Pederson, A.Sangiovanni-Vincentelli, "SPICE 3B1 User's Guide", Electronics Research Lab., U.C.Berkeley, Nov. 1987

[4] C.Turchetti, P.Mancini, G. Masetti, "A CAD-Oriented Non-Quasistatic Approach for the Transient Analysis of MOS IC's", IEEE JSSC Vol.SC-21, No.5, pp.827-836, 1986

[5] M.Bagheri, Y.Tsividis, "A Small Signal dc-to-High Frequency Nonquasistatic Model for the Four-Terminal MOSFET Valid in All Regions of Operation", IEEE Trans. Electron Devices, Vol. ED-32, No.11, pp. 2383-2391, 1985

[6] H.J.Park, P.K.Ko, C.Hu, "A Non-Quasistatic MOSFET Model for SPICE", IEDM 87 Technical Digest, pp.652-655, Dec. 1987

[7] H.J.Park, P.K.Ko, C.Hu, "A Non-Quasi-Static MOSFET Model for SPICE - Transient Analysis", IEEE Trans. Electron Devices, vol. ED-36, no.3, pp.561-576, Mar. 1989

[8] H.J.Park, P.K.Ko, C.Hu, "A Measurement Based Charge Sheet Capacitance Model of Short Channel MOSFETs for SPICE", IEEE IEDM 86 Technical Digest, pp.40-43, Dec. 1986

[9] L.W.Nagel, "SPICE2: A Computer program to Simulate Semiconductor Circuits", ERL-Memo, M520, 9 May 1975, Electronics Research Lab., University of California, Berkeley, CA 94720

[10] E.Cohen, "Program Reference for SPICE2", ERL Memo. ERL-M592, 1976, University of California, Berkeley

[11] K.Mayaram, "CODECS: A Mixed-Level Circuit and Device Simulator", Memorandum no. UCB/ERL M88/71, Electronics Research Lab., University of California, Berkeley, Nov. 21, 1988

[12]. P.Li, M.Chin, P.R.Gray, R.Castello, "Ratio-Independent Algorithmic Analog-to-Digital Conversion Techniques", IEEE Journal of Solid State Circuits, SC-19, pp.828-836, 1984

[13] P.R.Gray, R.G.Meyer, "MOS Operational Amplifier Design - A Tutorial Overview", IEEE JSSC, Vol.SC-17, No.6, pp.969-982, Dec. 1982

Appendix

(1) DC and AC analysis of a folded cascode CMOS OP Amp [13] (Fig.1,23)

```
One Stage Folded Cascode CMOS OP Amp (DC and AC analysis)
*
M0  3 15 20 20 pch w=10u   l=3u ad=36p as=36p pd=18u ps=18u
M1  4  1  3 20 pch w=50u   l=3u ad=36p as=36p pd=18u ps=18u
M2  5  2  3 20 pch w=50u   l=3u ad=36p as=36p pd=18u ps=18u
M3  8  9  4 30 nch w=9.14u l=3u ad=36p as=36p pd=18u ps=18u
M4 10  9  5 30 nch w=9.14u l=3u ad=36p as=36p pd=18u ps=18u
M5  6  6 20 20 pch w=20u   l=3u ad=36p as=36p pd=18u ps=18u
M6  7  6 20 20 pch w=20u   l=3u ad=36p as=36p pd=18u ps=18u
M7 10  8  6 20 pch w=20u   l=3u ad=36p as=36p pd=18u ps=18u
M8  8  8  7 20 pch w=20u   l=3u ad=36p as=36p pd=18u ps=18u
M9  5 11 30 30 nch w=30u   l=3u ad=36p as=36p pd=18u ps=18u
M10 4 11 30 30 nch w=30u   l=3u ad=36p as=36p pd=18u ps=18u
Vin1 1 0 AC 0.5 DC 0
Vin2 2 0 AC -0.5 DC 0
Vbias1 15 0 DC 4.55
Vbias2 11 0 DC -5.88
Vbias3 9 0 DC -2
Vdd 20 0 DC  8
Vss 30 0 DC -8
CL 10 0 4pF
.AC  DEC 20 100 100GIGA
.PRINT AC  VDB(10) VP(10)
.dc Vin1 -0.05 0.02 0.0002
.print dc v(10)
* model parameters
***** 3u n-channel mosfet *****
.model nch     nmos level=5
+  vto=0.9       kp=30.0u      gamma=1.36     phi=0.747
+  cgso=520p     cgdo=520p     rsh=20
+  cj=320u       mj=0.5        cjsw=900p      mjsw=0.33
+  js=100u       tox=50n       nsub=2.5e16    tpg=+1
+  xj=400n       ld=400n       uo=450         ucrit=80k
+  uexp=0.15     utra=0.3      vmax=50k
+  qtrtol=30     mintol=1.0
***** 3u p-channel mosfet *****
.model pch     pmos level=5
+  vto=-0.9      kp=15.0u      gamma=0.59     phi=0.66
```

```
+ cgso=400p     cgdo=400p     rsh=95
+ cj=200u       mj=0.5        cjsw=450p     mjsw=0.33
+ js=100u       tox=50n       nsub=5e15     tpg=-1
+ xj=400n       ld=500n       uo=200        ucrit=80k
+ uexp=0.15     utra=0.3      vmax=50k
+ qtrtol=30     mintol=1.0
*****
.opt acct
.end
```

(2). Turn-off transient of an NMOS pass transistor (Fig.4)

```
turn-off transient of a NMOS pass transistor
m1 1 2 3 4 enh w=20u l=3u ad=22p as=22p pd=20u ps=20u
Cs 3 0 2pF
Vg 2 0 dc 5 pwl 0 5 100p 0 1 0
.tran 1p  5n
Vb 4 0 dc 0
vin 11 0 dc 0
r1 1 11 10k
c1 1 0 2pF
.ic v(3)=0 v(11)=0
.print tran v(3)
.opt acct reltol=1e-6
.model enh nmos level=5 vto=1.13 tox=0.050u nsub=2.5e16 u0=800
+ ld=0.4u gamma=1.34 phi=0.75 nfs=5e10 vmax=85k neff=2
+ cgso=276p cgdo=276p cj=320u mj=0.5 cjsw=900p  mjsw=0.33
+ js=100u       tpg=+1        xj=200n
.end
```

(3) Differential sample-hold circuit [12] (Fig.5)

```
Sample and Hold Circuit for MOS A/D Converter
M1 1  20 2 50 nch w=200u l=3u ad=1200p as=1200p
M2 3  30 4 50 nch w=200u l=3u ad=1200p as=1200p
M3 5  20 6 50 nch w=200u l=3u ad=1200p as=1200p
M4 7  30 8 50 nch w=200u l=3u ad=1200p as=1200p
M5 2  40 6 50 nch w=200u l=3u ad=1200p as=1200p
C1 2 3  1.0pF
C2 3 4  1.0pF
C3 6 7  1.0pF
C4 7 8  1.0pF
```

```
*
*OP amp with differential input and output
* pos. inp.  (7)     neg. inp. (3)
* pos. out.  (4)     neg. out. (8)
* DC gain 10000(80dB)
* Unity gain freq.  3.2GHz
Eop1 9 0 7 3 5000
Rop1 9 4 100k
Cop1 4 0 5pF
Eop2 10 0  7 3 -5000
Rop2 10 8 100k
Cop2 8  0  5pF
*
* Voltage Sources
Vp1 20 0 pulse -5 5  0  1n 1n 9n 20n
Vp2 30 0 pulse -5 5  0  1n 1n 9n 20n
Vp3 40 0 pulse -5 5 11n 1n 1n 7n 20n
Vbb 50 0 dc -5
VinP 1 0 dc  0.5 sin ( 0.5  1.0 25MEG -30n 0)
VinM 5 0 dc -0.5 sin (-0.5 -1.0 25MEG -30n 0)
.tran 0.1n 40n  uic
.print tran v(1,5)
.print tran v(2,6)
.print tran v(4,8)
.opt acct
***** 3u n-channel mosfet *****
.model nch     nmos level=5
+  vto=0.9        kp=30.0u       gamma=1.36     phi=0.747
+  js=100u          tox=50n        nsub=2.5e16    tpg=+1
+  xj=400n        ld=400n        uo=450         ucrit=80k
+  uexp=0.15      utra=0.3       vmax=50k
***** 3u p-channel mosfet *****
.model pch     pmos level=5
+  vto=-0.9       kp=15.0u       gamma=0.59     phi=0.66
+  js=100u        tox=50n        nsub=5e15      tpg=-1
+  xj=400n        ld=500n        uo=200         ucrit=80k
+  uexp=0.15      utra=0.3       vmax=50k
.end
```